International Immunopharmacology 67 (2019) 78–86

Contents lists available at ScienceDirect

International Immunopharmacology

journal homepage: www.elsevier.com/locate/intimp

# Pseudoginsenoside-F11 attenuates cognitive impairment by ameliorating oxidative stress and neuroinflammation in D-galactose-treated mice

Zhen Zhang, Hanlin Yang, Jingyu Yang, Jun Xie, Jiaoyan Xu, Chen Liu, Chunfu Wu*

*Department of Pharmacology, Shenyang Pharmaceutical University, Shenyang, PR China*

ARTICLE INFO

*Keywords:*
Mild cognitive impairment
Pseudoginsenoside-F11
Oxidative stress
Neuroinflammation
D-Galactose

ABSTRACT

Oxidative stress and neuroinflammation are thought to be the two key early events during the process of mild cognitive impairment (MCI). Therefore, effective regulation of oxidative stress and neuroinflammation is an important aspect of preventing and improving MCI. We previously found that pseudoginsenoside-F11 (PF11), an ocotillol-type saponin, markedly reduced cognitive impairment in APP/PS1 mice and oA$\beta_{1-42}$-injected mice. In the present study, we further evaluate the effect of PF11 on learning and memory dysfunction in D-galactose (D-gal)-treated mice model of MCI. C57BL/6 mice received daily subcutaneous injections of D-gal (100 mg/kg) and oral administration of PF11 (2, 4, 8, 16 mg/kg) for 9 weeks. We observed that PF11 significantly alleviated D-gal-induced cognitive impairment, attenuated the loss of neuron and the over-activation of microglia in hippocampus of D-gal-treated mice. The elevated levels of nod-like receptor protein 3 (NLRP3) inflammasome in hippocampus of D-gal-treated mice were reduced by PF11 through reducing the accumulation of advanced glycation endproducts (AGEs) and the expression of the receptor of advanced glycation endproducts (RAGE). Moreover, PF11 significantly decreased $H_2O_2$ and malondialdehyde (MDA) levels, improved superoxide dismutase (SOD) activity and increased glutathione (GSH) level in D-gal-treated mice. Finally, D-gal treatment reduced the level of nuclear factor erythroid-related factor 2 (Nrf2) and glutathione S-transferase (GST) in hippocampus, which could reverse by PF11. Together, our findings indicated that PF11 exerts a protective effect against MCI-like pathological changes.

## 1. Introduction

Clinically, mild cognitive impairment (MCI) as a transitional state between the cognitive decline in normal aging and early features of Alzheimer's disease (AD) is thought to the appropriate stage for preventing or modifying progressive degeneration in AD [1,2]. Mounting evidence demonstrated that oxidative stress and neuroinflammation are the main early pathological features in MCI [3,4]. Excessive reactive oxygen species (ROS) can directly react with redox-sensitive biomolecules leading to neurodegeneration [3,5]. In addition, ROS promote the assembly of nod-like receptor protein 3 (NLRP3) inflammasome by aggravating the accumulation of advanced glycation endproducts (AGEs) and the expression of the receptor of advanced glycation endproducts (RAGE). Activation of NLRP3 inflammasome play a key role in maturity and release of interleukin-1β (IL-1β), which eventually lead to neuroinflammation and exacerbate neurodegeneration [6,7]. Therefore, effective regulation of oxidative stress and neuroinflammation is expected to be more efficient treatment strategy for MCI.

D-Galactose (D-gal) could be metabolized as a reducing sugar by aldose reductase in polyol pathway at high concentration. Several studies have revealed that D-gal can decrease glutathione (GSH) level and superoxide dismutase (SOD) activity [8], and increase malondialdehyde (MDA) levels by disturbing nuclear factor erythroid 2-related factor 2 (Nrf2) and antioxidative response elements (ARE) pathway in rodent [9,10], all of which are similar to the manifestations of clinical MCI patients. Thus, D-gal-treated mice have been widely used as a mimic cognition decline animal model for pharmacological intervention research of cognitive impairment [11–14].

Pseudoginsenoside-F11 (PF11), an ocotillol-type saponin found in *Panax quinquefolium* L. (American ginseng). We previously found that

*Abbreviations:* AD, Alzheimer's disease; AGEs, advanced glycation endproducts; AR, aldose reductase; ARE, antioxidative response elements; D-gal, D-galactose; GSH, glutathione; GST, glutathione S-transferase; MCI, mild cognitive impairment; MDA, malondialdehyde; MWM, Morris water maze; NLRP3, nod-like receptor protein 3; NOL, novel object location test; Nrf2, nuclear factor erythroid-related factor 2; PF11, pseudoginsenoside-F11; RAGE, receptor of advanced glycation endproducts; ROS, reactive oxygen species; SOD, superoxide dismutase

* Corresponding author.
*E-mail address:* wucf@syphu.edu.cn (C. Wu).

https://doi.org/10.1016/j.intimp.2018.11.026
Received 6 September 2018; Received in revised form 24 October 2018; Accepted 16 November 2018
Available online 08 December 2018
1567-5769/ 

PF11 significantly improved nesting-building activity, reduced working memory decline, mitigated spatial learning and memory impairment, and inhibited the expressions of β-amyloid precursor protein (APP) and $A\beta_{1-40}$ in the cortex and hippocampus in APP/PS1 mice and $oA\beta_{1-42}$-injected mice [15]. Moreover, PF11 alleviated the microglial activation and proinflammatory factors expression in both cortex and hippocampus in mice injected LPS [16], attenuates neuronal injury induced by cerebral ischemia or methamphetamine in experimental animals [17,18], indicating its benefit for several cognition decline. However, whether PF11 can ameliorate oxidative stress and disrupt activation of NLRP3 inflammasome to improve cognition ability has not been reported.

Thus, the present study was designated to evaluate the effect of PF11 on learning and memory dysfunction in D-gal-treated mice and its possible mechanism on oxidative stress and neuroinflammation. The results indicated that oral treatment of PF11 attenuates D-gal-induced cognitive impairment in a dose-dependent manner. The possible mechanism of PF11 may at least base on attenuating oxidative stress and lightening inflammatory response by promoting Nrf2/ARE pathway and attenuating NLRP3 inflammasome activation.

## 2. Material and methods

### 2.1. Animals

5–6 weeks old male C57BL/6 mice (18–22 g) were purchased from Beijing HFK Bioscience Co., Ltd. Animals were housed in standardized environment condition (12 h alternating light and dark, 22 ± 2 °C). All experiments were performed according to relevant guidelines and regulations approved by the Experimental Animal Research Committee of Shenyang Pharmaceutical University. All efforts were made to minimize suffering and to reduce the number of animals used.

### 2.2. Chemicals and drug treatments

D-Gal (99%) was purchased from Amesco Co., Ltd. (OH. USA). PF11 was isolated from the aerial parts of P. quinquefolium by the Department of Chemistry for Natural Products of Shenyang Pharmaceutical University (China). The purity was > 98% as determined by HPLC. PF11 (2, 4, 8, 16 mg/kg) and Donepezil (5 mg/kg) were dissolved in distilled water and orally given daily after subcutaneous injection of D-gal (100 mg/kg). The treatment lasts for nine weeks. Donepezil is a classic drug used to treat MCI in clinical, and the dose we chose is the clinical equivalent of the largest drug dose used to treat MCI [19,20].

### 2.3. Novel object location test (NOL)

The experiment was comprised of a habituation phase, an acquisition phase and a recognition test [21]. Three experimental phases were separated by a 24 h delays and each phase was recorded by a video-tracking system EthoVision (Noldus, Wageningen, NL). In habituation phase, each mouse was placed in the empty black plastic box and allowed to move freely for 5 min. In the acquisition phase, two similar objects (A1 and A2) were placed near the corner of the same wall. Each mouse was placed into the apparatus facing the opposite wall which objects are located and allowed to explore for 5 min. In recognition test, one of two similar objections were placed in opposite position of the original position. Exploration behavior was defined as mouse directing its nose toward the object within 2 cm. The discrimination index was calculated as exploration novel object time/total exploration time.

### 2.4. Y maze test

Y maze was made of three black-painted wooden arms (40 × 12 × 3 cm) radiating out from the center compartment [22]. Each mouse was placed in the center compartment and allowed free exploration of the maze for 8 min. Before each trail, 75% alcohol was used to eliminate odors from previously mouse and each mouse performed one trial. The sequence of arm entries was manually recorded. Spontaneous alteration was defined as entry into three arms in successively order. Spontaneous alteration behavioral (%) was calculated as actual alterations/total number of arm entries.

### 2.5. Morris water maze test

Morris water maze was made of circle polypropylene pool (120 × 40 cm) filled with white-opaque water (23 ± 1 °C). The pool was equally divided into four quadrants and a transparent platform (9 cm) was submerged 1 cm below the water surface at target quadrant. Some visual cues helping mice to locate the hidden platform were placed surrounding the maze [23]. The procedure of MWM test contained a consecutive five-day navigation phase and a one-day probe phase. In the navigation phase, each mouse was allowed to locate the hidden platform for 90 s. Time spent to find the platform was defined as escape latency. Escape latency (s) was recorded and each mouse was received three trials per day. Mice failing to search the platform within 90 s were placed manually on the platform and stayed there for 10 s, and its escape latency was recorded as 90 s. In the probe phase, the hidden platform was removed from pool and each mouse received a free swimming of 60 s' duration. Time spent in the target quadrant and number of platform crossings were measured. All data were recorded and calculated by a video-tracking system EthoVision (Noldus, Wageningen, NL).

### 2.6. Preparation of tissue samples

The mice were anesthetized by intrapulmonary injection of 4% chloral hydrate after behavioral analysis, and perfumed transversally with 40 ml ice-cold 0.9% saline. Brain tissues were detached and separated into two parts through the midsagittal plane. The hippocampus and cortex separated from the left hemisphere was collected immediately and stored at −80 °C for commercial kits analysis and western blotting. The right hemisphere was fixed in 4% paraformaldehyde (pH 7.4) overnight and cryoprotected in 30% sucrose prepared in PBS, and embedded in Optimal Cutting Temperature (OCT, Leica, CA, Germany). Serial coronal cryosections (20 μm) were cut using freezing microtome and stored at −40 °C for Nissl staining.

### 2.7. Transmission electron microscope (TEM)

Upon anesthesia, the mice were perfused transcardially with ice cold saline solution followed by 4% paraformaldehyde ~2.5% glutaraldehyde solution. Brains were immediately isolated and hippocampus CA1 was post-fixed in 2.5% glutaraldehyde at 4 °C for ultra-structure observation of synapses using transmission electron microscope.

### 2.8. Assay of the activity of AR

AR activity was measured through the method reported previously [24]. Briefly, the reaction system contains 0.3 mM NADPH, 0.1 M PBS, 0.4 M Lithium sulfate, 1.25 mM D,L-glyceraldehyde, 0.1 M β-mercaptoethanol and AR supernatant (crude AR solution). All solutions were volleyed and incubated at 37 °C for 10 min. The decrease of NADPH absorbance at 340 nm was monitored continuously for 5 min. One unit (U) of AR activity was defined as the decrease of absorbance per min induced by 1 mg protein.

### 2.9. AR enzyme-linked immunosorbent assay

The hippocampus and prefrontal cortex tissues of the left hemisphere were homogenized with 0.9% saline at a ratio of 1:10, and

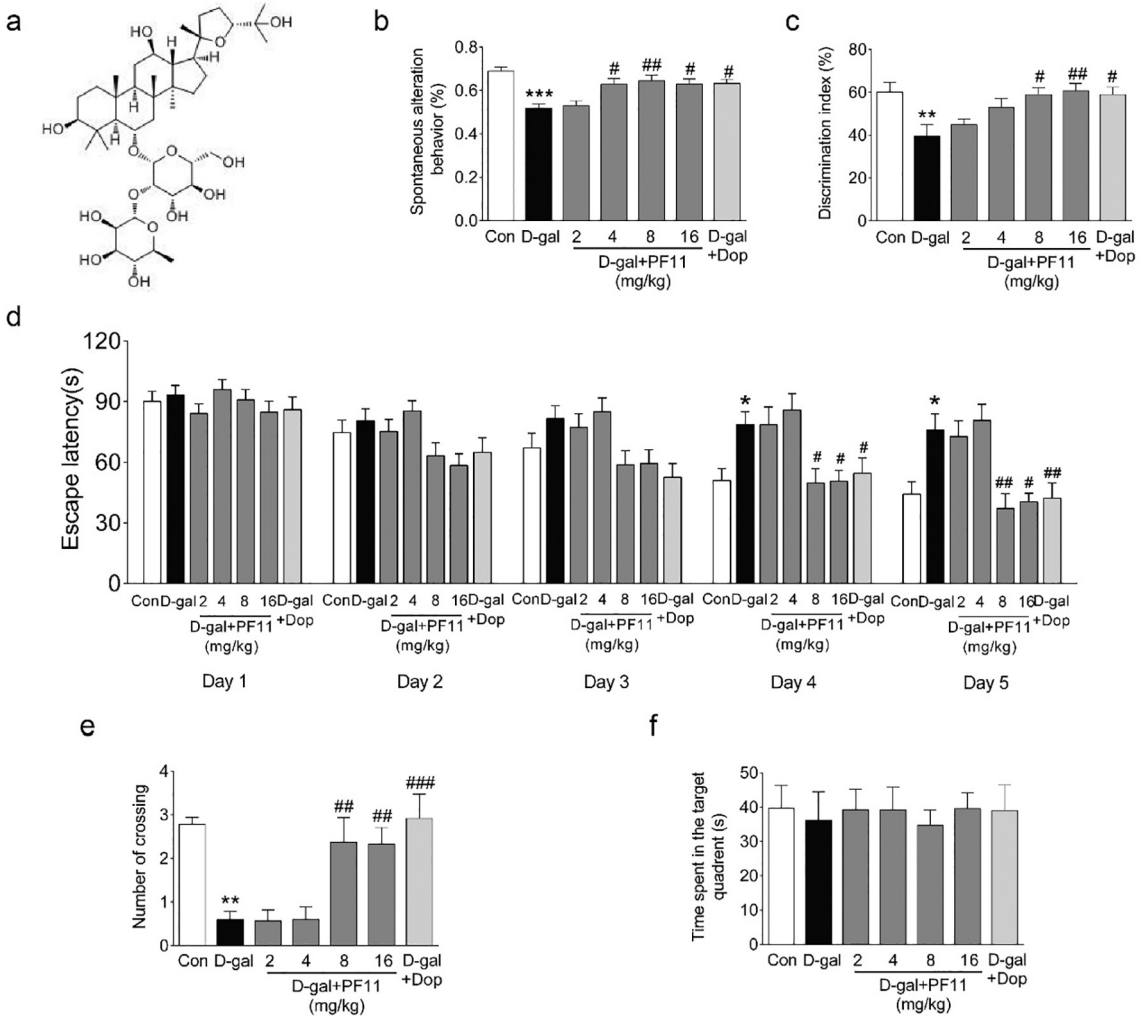


**Fig. 1.** Pseudoginsenoside-F11 ameliorated cognitive impairment in D-galactose-treated mice.
Chemical structure of pseudoginsenoside-F11 (PF11) (A) (C42H72O14, molecular weight = 801.02). Graphs show the effect of PF11 working memory in Y maze and NOL test (B, C), performance in the Morris water maze (D–F). PF11 significantly improves several cognitive impairment behaviors induced by D-galactose treatment. Data are expressed as means ± SEM (n = 12–15 mice/group). Statistical analysis was performed with one-way ANOVA, followed by the Tukey test *P < 0.05, **P < 0.01 and ***P < 0.001 vs vehicle. #P < 0.05, ##P < 0.01 and ###P < 0.001 vs D-galactose model.

centrifuged at 12000*g* for 10 min. The supernatants were collected for quantified analysis by ELISA kits (Shanghai Enzyme-linked Biotechnology Co. Ltd. China), following the manufacturer's instructions.

### 2.10. Assay the activity of SOD and the level of $H_2O_2$, MDA and GSH

The supernatants of the hippocampus and cortex were collected after homogenizing with ice-cold 0.9% saline and centrifuging at 4000*g* for 15 min. The activity of SOD and the level of $H_2O_2$, MDA and GSH were measured using commercial assay kits (Beyotime, China) according to the manufacturer's instructions.

### 2.11. Nissl staining

Cornel cryosections were subjected to Nissl staining. Briefly, the sections were washed in PBS three times and stained with Nissl staining solution (Beyotime, China) for 1 h at 70 °C. Then, the sections were washed in PBS, dehydrated in gradient ethanol, and coverslipped using glass slides. Sections were viewed and imaged under a light microscopy.

### 2.12. Western blotting

The hippocampus of left hemisphere was cryohomogenized in RIPA lysis buffer (Beyotime, China). The supernatants and sediments were obtained for the collection of nuclear and cytoplasmic proteins according to manufacturer's protocol (Beyotime, China). Tissue lysates were mixed with SDS-PAGE protein loading buffer and boiled for 5 min. Equal amounts of protein were separated by 8%–12% SDS-PAGE and transferred to polyvinylidene fluoride membrane (PVDF). The membranes were blocked in 5% milk or BSA for 60 min and then incubated with correspondent primary antibody against NLRP3 (1:500; CST), caspase-1(1:1000; Abcam), glutathione S-transferase (GST) (1:1000; Abcam), Nrf2(1:500; Abcam), IL-1β (1:1000; Abcam), RAGE (1:500; Abcam), AGEs (1:500; Abcam), Lamin B (1:2000; Sigma) and β-actin (1:1000; Santa Cruz Biotechnology) overnight at 4 °C. After repeated washing in Tris-buffered Saline-Tween 20 (TBST), the corresponding second antibodies were applied to the membrane for 1 h at room temperature. The bands were visualized by the enhanced chemiluminescence (ECL) (Thermo. USA) and were analyzed with ImageJ software.

### 2.13. Immunohistochemistry

Cornel cryosections were washed in PBS and received a microwave

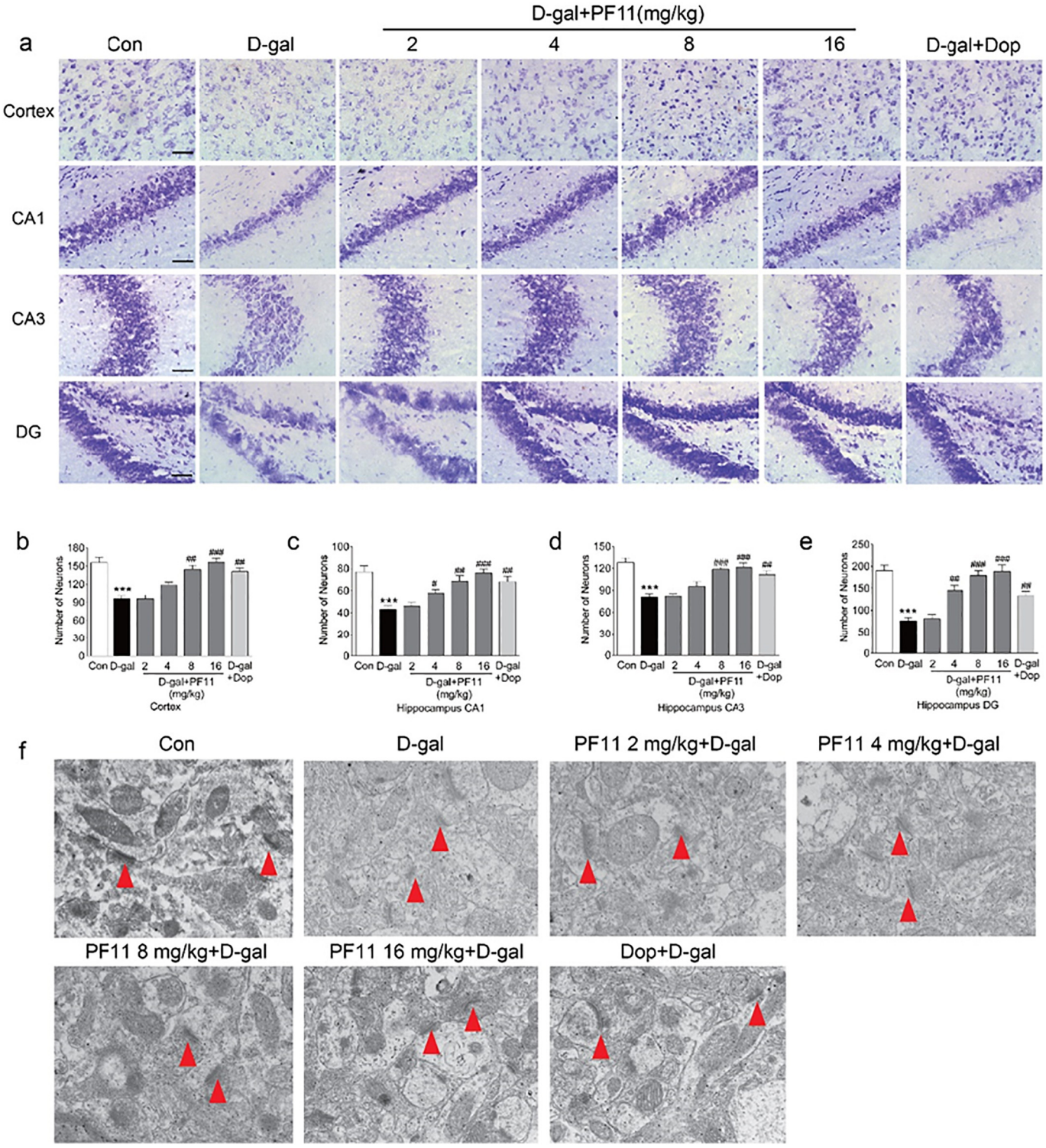


**Fig. 2.** Pseudoginsenoside-F11 attenuated the loss of neuron and postsynaptic density in D-galactose-treated mice.
Nissl-staining images showing that PF11 significantly reversed the D-galactose-induced neuron loss in the hippocampus and cortex (a). Scale bars: 50 μm. Graphs show the number of Nissl-dying neuron (b–e) in the D-galactose-treated mice. Statistical analysis of surviving neurons (Nissl-dying neuron) was conducted using Image-Pro Plus 6.0. The data are presented as means ± SEM (n = 12) Transmission electron microscopy (TEM) representative images of tissues from the hippocampus (f). The red arrows indicate a region of postsynaptic density. Statistical comparisons were carried out with ANOVA followed by Tukey's test. **P < 0.01 and ***P < 0.001 vs vehicle. #P < 0.05, ##P < 0.01 and ###P < 0.001 vs D-galactose model. (For interpretation of the references to color in this figure legend, the reader is referred to the web version of this article.)

treated antigen retrieval. Next, sections were quenched with 3% hydrogen peroxide for 20 min, and then incubated in blocking solution to prevent nonspecific binding of IgG for 1 h at 37 °C. Subsequently, the primary antibody including Iba-1 (1:500; Sigma), NeuN (1:500; Millipore) was applied to the sections at 4 °C overnight. Negative control was incubated with PBS without primary antibody. After being washed thoroughly in PBST, sections were reacted with biotinylated secondary antibody and horseradish peroxidase in series for 1 h at

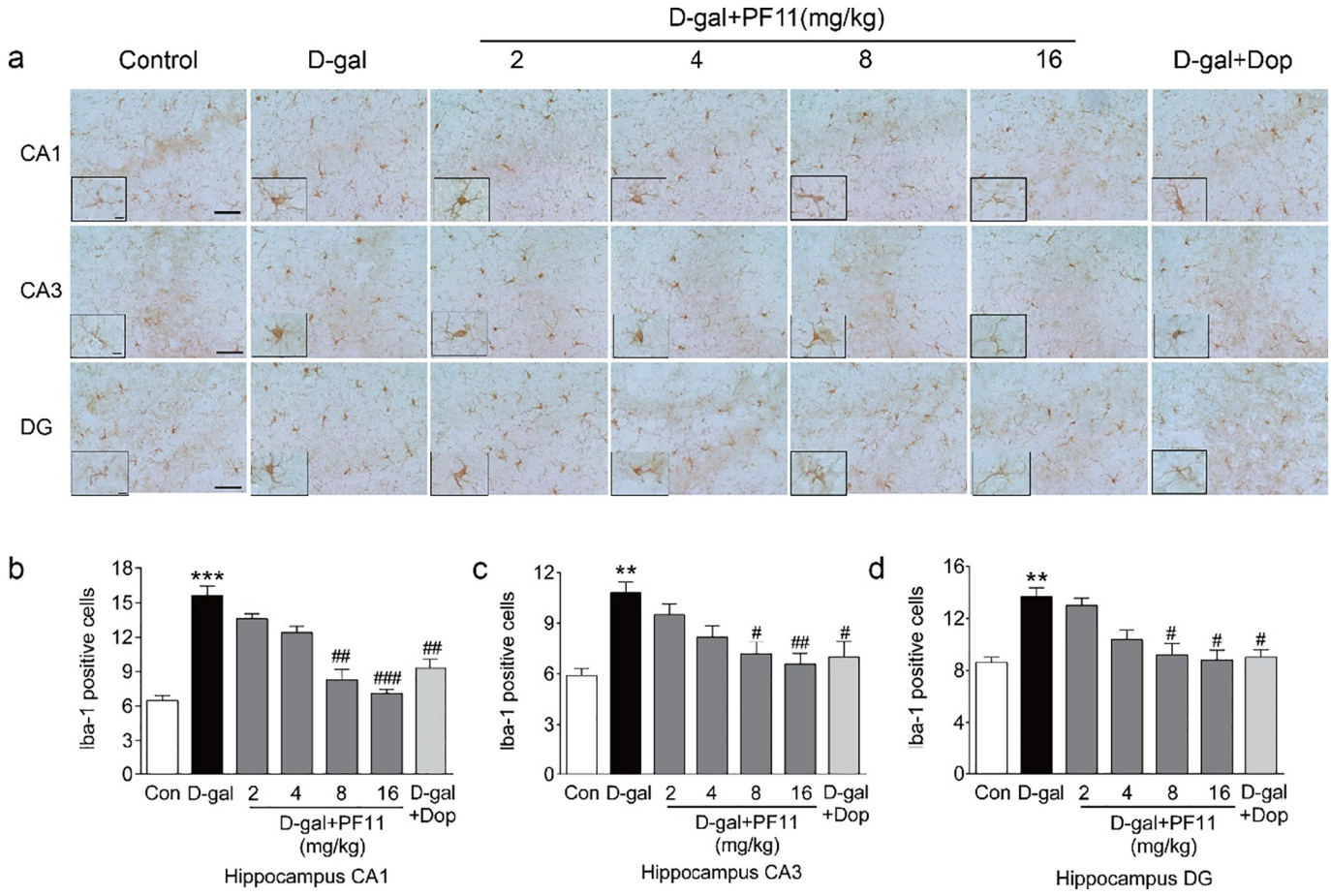


**Fig. 3.** Pseudoginsenoside-F11 attenuated the number of over-active microglia in D-galactose-treated mice.
Immunohistochemistry images showing that PF11 significantly reversed the D-galactose-induced microglial activation (a). The boundary between the gels is delineated by a black line. Graphs show the number of Iba-1 positive cell in hippocampus of different groups mice (b–d). High-magnification images of the boxed areas are shown in the inserts. Scale bars: 50 μm. Statistical comparisons were carried out with ANOVA followed by Tukey's test. Data are presented as means ± SEM (n = 12). **P < 0.01 and ***P < 0.001 vs vehicle. #P < 0.05, ##P < 0.01 and ###P < 0.001 vs D-galactose model.

37 °C. After incubation with 3,3-diaminobenzidine (DAB) for 5 min at 37 °C, the sections were washed in distilled water, and then were subjected to dehydration of gradient ethanol and mounted on glass slides. Finally, sections were observed and imaged using light microscopy. The number of immune positive cells was analyzed by Image pro plus 6.0 software.

### 2.14. Statistical analysis

All data were reported as means ± standard errors and analyzed by SPSS 21.0 statistical software.

For the behavioral tests, one-way ANOVA was used to compare the differences among groups with Tukey's test; and escape latency in the Morris water maze test navigation phase were analyzed by two-way analysis of variance (ANOVA) with repeated measures. The level of significance was set at $P < 0.05$.

For western blotting, immunohistochemistry, Nissl-staining and TEM, one-way ANOVA was used to compare the differences among groups with Tukey's test. The level of significance was set at $P < 0.05$.

## 3. Results

### 3.1. PF11 ameliorated cognitive impairment in D-gal-treated mice

To investigate the effect of PF11 on cognition decline in D-gal-treated mice, a series of cognition-related behavior tests were performed. D-Gal induced a noticeable reduction of spontaneous alternation percentage (0.52 ± 0.02, $P < 0.001$, $F = 7.027$) (Fig. 1b) and the discrimination index in NOL (39.6 ± 5.43, $P < 0.01$, $F = 4.584$) (Fig. 1c) compared to vehicle-treated mice. PF11 (8, 16 mg/kg) and Donepezil significantly elevated the spontaneous alternation percentage (0.62 ± 0.03, $P < 0.05$; 0.64 ± 0.03, $P < 0.01$; 0.63 ± 0.02, $P < 0.05$), and increased discrimination index (59.0 ± 3.23, $P < 0.05$; 60.7 ± 3.46, $P < 0.01$; 59.0 ± 3.34, $P < 0.05$) (Fig. 1b–c). MWM test indicated that D-gal lengthened escape latency (85.9 ± 7.97, $P < 0.05$, $F = 9.069$) (Fig. 1d) on day 5 of navigation test, and decreased the number of platforms crossing in probe test (0.60 ± 0.19, $P < 0.05$, $F = 7.929$) (Fig. 1e). PF11 (8, 16 mg/kg) reduced the escape latency (37.2 ± 7.37, $P < 0.05$; 40.4 ± 4.26, $P < 0.05$) (Fig. 1d) and increased the number of platforms crossing (2.37 ± 0.57, $P < 0.01$; 2.33 ± 0.38, $P < 0.05$) (Fig. 1e) in probe test, and Donepezil has a similar effect on escape latency and the number of platforms crossing (Fig. 1d–e). In addition, no difference was found in time spent in the target quadrant among different groups (Fig. 1f). Taken together, these results indicated that PF11 significantly ameliorated cognitive impairment in D-gal-treated mice.

### 3.2. PF11 attenuated neuronal damage in D-gal-treated mice

Next, we choose Nissl-staining to determine the extent of neurodegeneration in D-gal-treated mice. As shown in Fig. 2A, the number of Nissl-positive neuron was reduced in memory-associated hippocampus

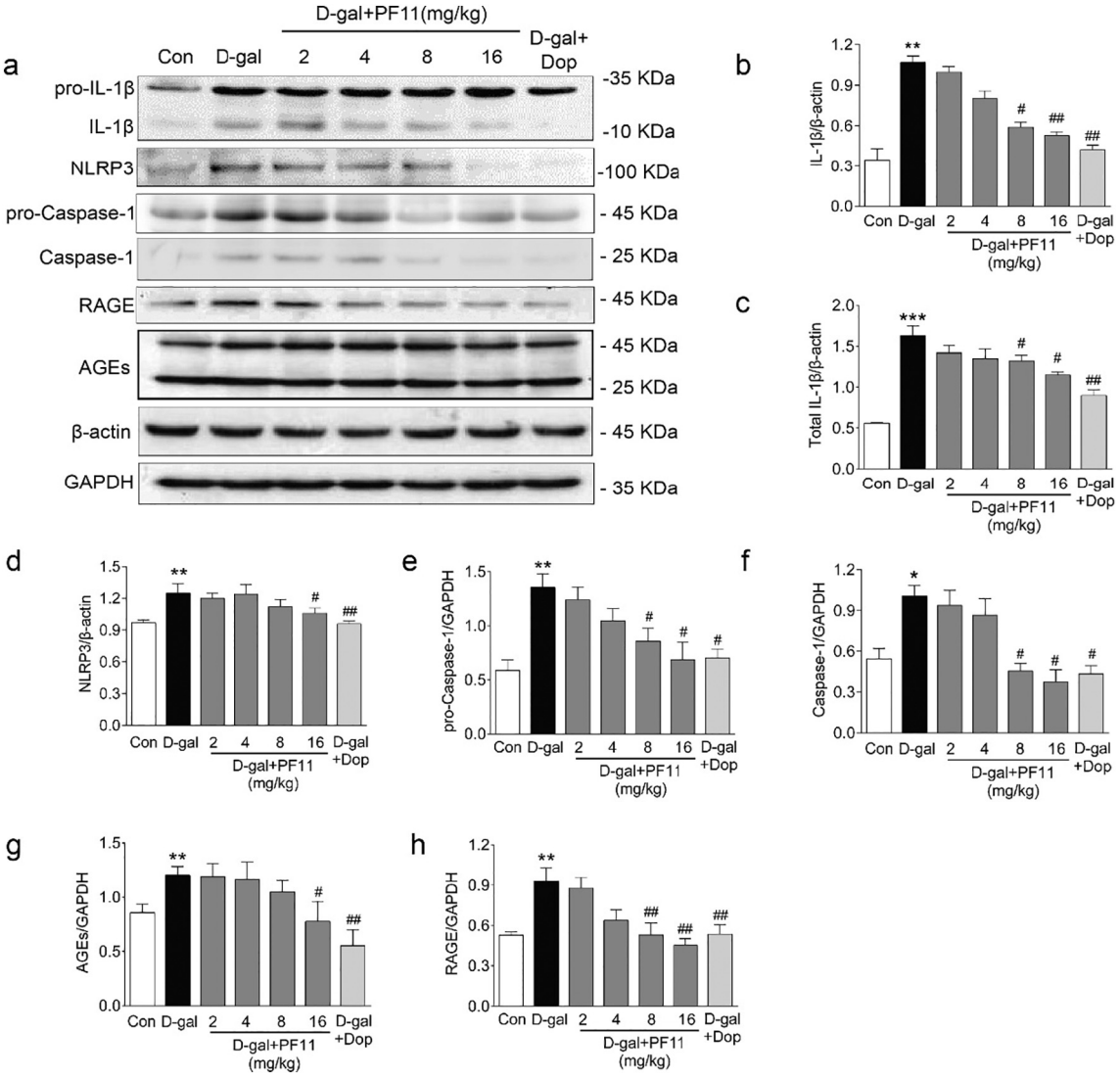


**Fig. 4.** Pseudoginsenoside-F11 attenuated neuroinflammation in D-galactose-treated mice.
(a) Western blot analysis of pro- interleukin (IL)-1β, IL-1β, nod-like receptor protein 3 (NLRP3), pro-caspase-1, caspase-1, advanced glycation endproducts (AGEs) and the receptor of advanced glycation endproducts (RAGE) levels in hippocampus among different groups. β-Actin and GAPDH were used as a loading control. (b–h) Quantitative analysis of the immunoblotted proteins was performed with ImageJ. Statistical comparisons were carried out with ANOVA followed by Tukey's test. Data are presented as means ± SEM (n = 6). **P < 0.01 and ***P < 0.001 vs vehicle. #P < 0.05, ##P < 0.01 and ###P < 0.001 vs D-galactose model.

and cortex. In contrast, PF11 and Donepezil can reduce the number of neurons in the corresponding area (Fig. 2b–e). TEM results indicated that D-gal thinned postsynaptic density while PF11 (4, 8, 16 mg/kg) reversed this change. These results showed that PF11 attenuated neuronal damage against D-gal-induced neurotoxicity.

### 3.3. PF11 attenuated the neuroinflammation in D-gal-treated mice

To investigate whether neuroprotective effect of PF11 was associated with the inhibition of the inflammatory response, the degree of microglia activation, the expression of interleukin (IL)-1β and NLRP3 inflammasome-related proteins were measured. As shown in Fig. 3a, the number of Iba-1-positive microglia was significantly increased in hippocampus of D-gal-treated mice. Western blotting analysis also showed that D-gal-treated mice had a higher level of IL-1β and NLRP3 inflammasome-related proteins such as NLRP3, pro-Caspase-1 and Caspase-1 (Fig. 4b–f). PF11 decreased the increasing number of active microglia (Fig. 3b–d), and normalized the expression of IL-1β and NLRP3 inflammasome-related protein in dose-dependent manner. Furthermore, AGEs/RAGE pathway has been reported to participate in the regulating of NLRP3 inflammasome activation [6]. It was observed that there was a significant increase of AGEs and RAGE in D-gal-treated mice. Notably, PF11 treatment attenuated the expression of AGEs and RAGE (Fig. 4g–h). All these results indicated PF11 attenuated D-gal-induced neuroinflammation, at least by disturbing the assembly of NLRP3 inflammasome.

### 3.4. PF11 attenuated oxidative stress in D-gal-treated mice

To investigate whether PF11 has an effect on oxidative stress, a series of redox classic markers was detected. As shown in Fig. 5a–d, D-gal treatment increased the $H_2O_2$ and MDA levels, decreased GSH level and SOD activity of both hippocampus and cortex, which were reversed by PF11 in a dose-dependent manner. It is reported that AR plays an important role in the production of ROS during the mechanism of D-gal [25,26]. As shown in Fig. 5e–f, the $IC_{50}$ value for PF11 on AR is 121.4 μM which was much higher than that of AR inhibitor Epalrestat ($IC_{50}$ = 0.218 μM) in vitro, while PF11 treatment did not change D-gal-induced abnormal increasing of AR ability in vivo (Fig. 5g). Moreover, the Nrf2/ARE pathway is necessary to maintain the redox balance

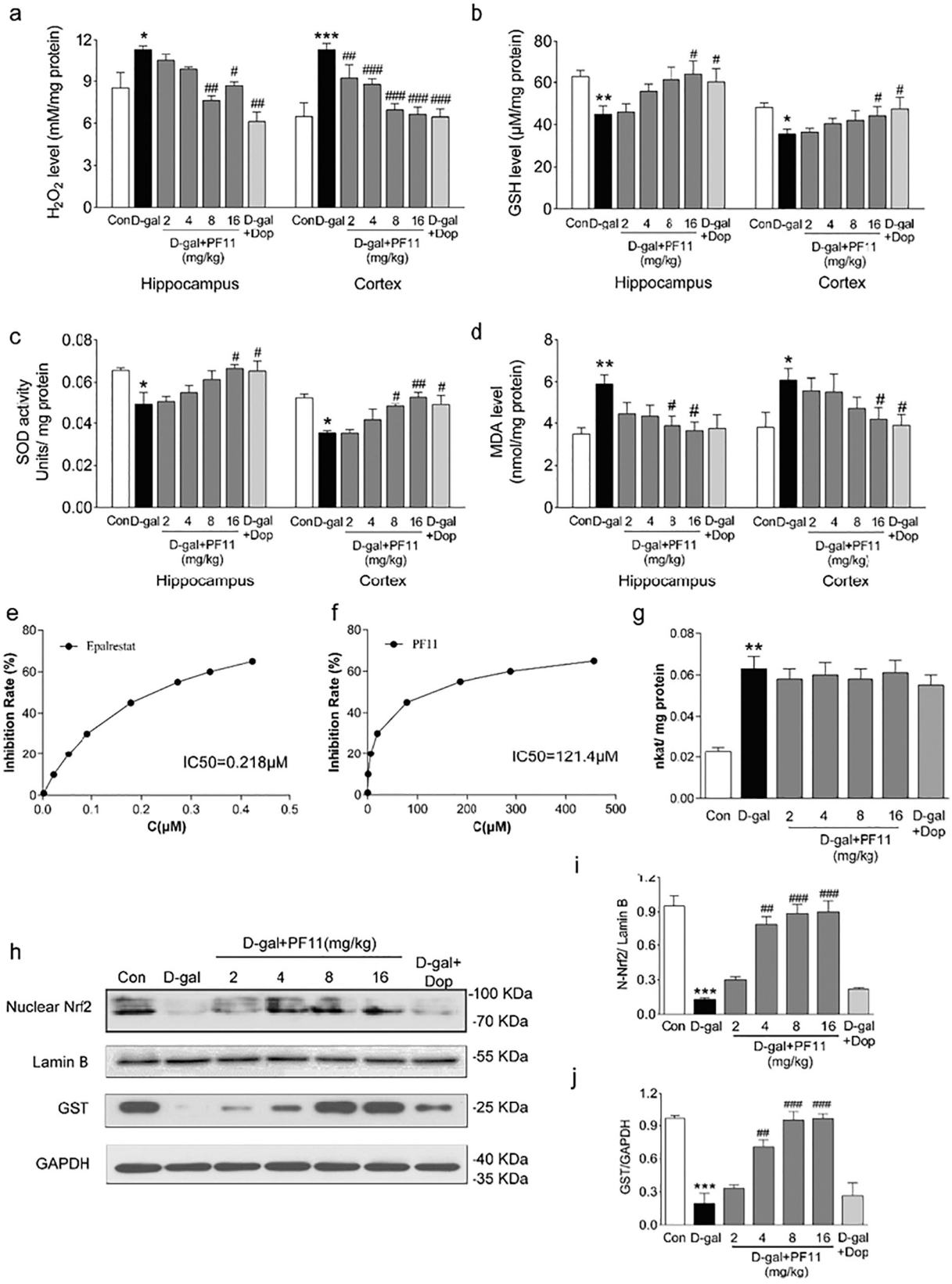


**Fig. 5.** Pseudoginsenoside-F11 restored the redox-state in D-galactose-treated mice.

The level of $H_2O_2$ (a), glutathione (GSH) (b) and malondialdehyde (MDA) (d), and the activity of superoxide dismutase (SOD) (c) were measured by kits. PF11 significantly increases the level of $H_2O_2$ and MDA, decreases the level of MDA, and enhances the activity of SOD in hippocampus and cortex of D-galactose-treated mice. The Epalrestat (e) and PF11 (f) inhibits aldose reductase (AR) in series of concentration in vivo. The effect of PF11 on AR in vivo are shown in (g). Western blot analysis of nuclear factor erythroid-related factor 2 (Nrf2) and glutathione S-transferase (GST) in hippocampus among different groups. Lamin-B and GAPDH were used as a loading control (h–j). Quantitative analysis of the immunoblotted proteins was performed with ImageJ. Statistical comparisons were carried out with ANOVA followed by Tukey's test. Data are presented as means ± SEM (n = 6). **P < 0.01 and ***P < 0.001 vs vehicle. #P < 0.05, ##P < 0.01 and ###P < 0.001 vs D-galactose model.

[27,28]. Western blotting results showed that nuclear Nrf2 and GST protein level in D-gal-treated mice was significantly lower than those in vehicle-treated mice (Fig. 5h), which were reversed by treatment of PF11 (Fig. 5i–j). Taken together, these results indicated that PF11 can attenuate D-gal-induced redox imbalance through facilitating nuclear accumulation of Nrf2 and enhancing the expression of GST.

## 4. Discussion

Our previously studies have demonstrated that PF11 has an extensive beneficial effect on several disorders of central nervous system. In the present study, we reported that PF11 exerts a protective effect against D-gal-induced cognitive impairment. Oral administration of PF11 (8, 16 mg/kg) for 9 weeks improves cognition abilities and ameliorates neuronal damage. Moreover, we found that NLRP3 inflammasome may be involved in D-gal-mediated inflammatory response, and PF11 attenuates D-gal-induced neuroinflammation at least partly through disturbing the assembly of the NLRP3 inflammasome. What's more, PF11 lightened oxidative stress in D-gal-treated mice by promoting Nrf2/ARE pathway. These results suggest that PF11 ameliorates progressive memory decline in D-gal-treated mice, and the potential mechanism may be associated with attenuating of oxidative stress and neuroinflammation.

D-gal-treated mice have several MCI-like cognitive impairment such as working memory and spatial memory dysfunction. In this manuscript, we chose Y maze test and NOL test (for detecting working memory), and MWM (for detecting spatial memory) to evaluate cognition of the D-gal-treated mice. Consistent with other reports, it was found that D-gal can reduce spontaneous alternation percentage, decrease the discrimination index, lengthen escape latency and shorten the time spent in the target quadrant [29–31]. Our results revealed that PF11 could improve spatial learning and memory performance, attenuate working memory decline, and ameliorate the deficits of organized behavior in D-gal-treated mice.

Normal cognitive abilities are based on a considerable number of neuron and natural synaptic function. In previous studies, the number of neurons was significantly decreased in the hippocampus CA3 region of D-gal-treated mice [9,22], and our data also showed that Nissl-dyeing neurons display a sharp reduction in the hippocampus and cortex in D-gal-treated mice, which was reversed by PF11. TEM results also indicated that PF11 prevents D-gal-induced thinning of postsynaptic dense in hippocampus of C57 mice.

Many studies have shown that neuroinflammation triggered by microglial activation and accumulation of inflammatory factors plays an important role in the cascade of MCI. It has been demonstrated that accumulation of IL-1β will aggravate neurodegeneration which can be rescued by blocking IL-1β signaling in APP/PS1 mice [32]. In line with previous studies [11,31], our results also showed that the number of active microglia and the level of IL-1β were increased in D-gal-treated mice. NLRP3 inflammasome is essential for caspase-1 activation, and the latter regulate the activation and release of IL-1β [33]. In recent study, it was reported that activation of NLRP3 inflammasome occurs in microglia in AD patients, which suggested that inhibition of NLRP3 could reduce AD pathology in vivo [34,35]. However, whether NLRP3 inflammasome implicated in D-gal-induced neuroinflammation has not been reported. In this study, we firstly observed increased level of NLRP3, pro-caspase-1 and caspase-1 in hippocampus of D-gal-treated mice, which are the components of NLRP3 inflammasome. And, PF11 can decrease those changes in a dose-dependent manner. These results indicated that PF11 may interfere with the assembly of NLRP3 inflammasome.

The assembly of the NLRP3 inflammasome requires a priming signal derived from pattern recognition or cytokine receptors followed by a second signal derived from pore forming toxins, extracellular ATP, or ROS [36]. AGEs/RAGE pathway has been demonstrated to mediate the activation of NLRP3 inflammatory by providing priming signal in transcriptional level [6,37]. Our results showed a higher level of AGEs and RAGE in hippocampus of D-gal-treated mice, which is decreased by PF11. In addition, D-gal could be metabolized to galactitol as a reducing sugar by AR in polyol pathway at high concentration [38]. Excessive activation of this process exhausts cytosolic NADPH, increases the accumulation of ROS, disrupts Nrf2/ARE pathway, finally leading to oxidative stress [39]. Importantly, growing evidence indicates that ROS is critical for AGEs accumulation [40]. Thus, we further examine whether the inhibition effect of PF11 on AGEs accumulation is dependent on reducing ROS. The results showed that D-gal treatment remarkably reduced the GSH level, caused the accumulation of $H_2O_2$ and MDA, decreased antioxidant enzyme activity such as SOD, and eventually triggered neurodegeneration. PF11 significantly reversed those changes in a dose-dependent manner indicting its benefit effects on oxidative stress.

AR play an important role in D-gal-triggered oxidative stress. We measured the effect of PF11 on AR activity in vivo and in vitro. The results showed that PF11 did not affect increased AR ability or protein level in D-gal-treated mice. Moreover, our previous study has demonstrated that PF11 has no direct clearance or capture effect on free radicals [16]. These results indicated that PF11 also have no effect on the production of ROS. Nrf2 has been shown to be a critical transcription factor which involved in the regulation of transcriptional levels of many antioxidants such as glutathione S-transferases GST, heme oxygenase 1 (HO-1) and NAD(P) H-quinone oxidoreductase 1(NQO1) [28]. Recent studies have reported that the decreased Nrf2 expression in AD animal and patients [41], and restoring the normal level of Nrf2 may be a new strategy for the treatment of AD and MCI. In a latest study, Nrf2/ARE is directly implicated in the regulation of inflammation rather than relying on regulating oxidative stress to control inflammatory response [42,43]. Our data showed a lower nuclear Nrf2 level and GST level in D-gal-treated mice, which notably enhanced by PF11. Taken together, PF11 ameliorate oxidative stress possibly by restoring Nrf2/ARE pathway. As a master regulator of the antioxidant response, the nuclear transport of Nrf2 is tightly regulated in the cell. Kelch-like ECH-associated protein 1 (Keap1) has been shown to interact with Nrf2 in cytoplasm under quiescent conditions, which will facilitate the ubiquitination and subsequent proteolysis of Nrf2 [44]. Whether PF11 increased the level of nuclear Nrf2 is dependent on the Keap1 requires further exploration.

In conclusion, we have shown that PF11 attenuated D-gal-induced cognitive impairment, oxidative stress and neuroinflammation by restoring Nrf2/ARE pathway. These benefit effects indicated that PF11 may be a potential new candidate for the treatment of MCI.

## Conflict of interest

All the authors declare that there is no conflict of interests regarding the publication of this paper.

## Declarations of interest

None.

## Acknowledgments

This research did not receive any specific grant from funding agencies in the public, commercial, or not-for-profit sectors.

## References

[1] E. Carro, et al., Early diagnosis of mild cognitive impairment and Alzheimer's disease based on salivary lactoferrin, Alzheimers Dement. 8 (2017) 131–138.
[2] R.C. Petersen, How early can we diagnose Alzheimer disease (and is it sufficient)? The 2017 Wartenberg lecture, Neurology 91 (9) (2018) 395–402.
[3] A. Garcia-Blanco, et al., Potential oxidative stress biomarkers of mild cognitive impairment due to Alzheimer disease, J. Neurol. Sci. 373 (2017) 295–302.

[4] S.W. Scheff, M.A. Ansari, E.J. Mufson, Oxidative stress and hippocampal synaptic protein levels in elderly cognitively intact individuals with Alzheimer's disease pathology, Neurobiol. Aging 42 (2016) 1–12.
[5] S.I. Mota, et al., Oxidative stress involving changes in Nrf2 and ER stress in early stages of Alzheimer's disease, Biochim. Biophys. Acta 1852 (7) (2015) 1428–1441.
[6] W.J. Yeh, et al., Long-term administration of advanced glycation end-product stimulates the activation of NLRP3 inflammasome and sparking the development of renal injury, J. Nutr. Biochem. 39 (2017) 68–76.
[7] R. Zhou, et al., A role for mitochondria in NLRP3 inflammasome activation, Nature 469 (7329) (2011) 221–225.
[8] A. Majdi, et al., Nicotine modulates cognitive function in D-galactose-induced senescence in mice, Front. Aging Neurosci. 10 (2018) 194.
[9] D.Y. Yoo, et al., Melatonin improves D-galactose-induced aging effects on behavior, neurogenesis, and lipid peroxidation in the mouse dentate gyrus via increasing pCREB expression, J. Pineal Res. 52 (1) (2012) 21–28.
[10] Y. Sang, et al., Apigenin exhibits protective effects in a mouse model of D-galactose-induced aging via activating the Nrf2 pathway, Food Funct. 8 (6) (2017) 2331–2340.
[11] X. Cui, et al., Chronic systemic D-galactose exposure induces memory loss, neuro degeneration, and oxidative damage in mice: protective effects of R-alpha-lipoic acid, J. Neurosci. Res. 84 (3) (2006) 647–654.
[12] S.C. Ho, J.H. Liu, R.Y.Y. Wu, Establishment of the mimetic aging effect in mice caused by D-galactose, Biogerontology 4 (1) (2003) 15–18.
[13] L. Hao, et al., The influence of gender, age and treatment time on brain oxidative stress and memory impairment induced by D-galactose in mice, Neurosci. Lett. 571 (2014) 45–49.
[14] S.-C. Hoi, Jue-Hao Liu, ReY-Yih Wu, Establishment of the mimetic aging effect in mice caused by d-galactose, Biogerontology 4 (2003) 15–18.
[15] C.M. Wang, et al., Anti-amnesic effect of pseudoginsenoside-F11 in two mouse models of Alzheimer's disease, Pharmacol. Biochem. Behav. 106 (2013) 57–67.
[16] X. Wang, et al., Pseudoginsenoside-F11 (PF11) exerts anti-neuroinflammatory effects on LPS-activated microglial cells by inhibiting TLR4-mediated TAK1/IKK/NF-kappaB, MAPKs and Akt signaling pathways, Neuropharmacology 79 (2014) 642–656.
[17] Y.Y. Liu, et al., Pseudoginsenoside-F11 attenuates cerebral ischemic injury by alleviating autophagic/lysosomal defects, CNS Neurosci. Ther. 23 (7) (2017) 567–579.
[18] K. Fu, et al., Pseudoginsenoside-F11 inhibits methamphetamine-induced behaviors by regulating dopaminergic and GABAergic neurons in the nucleus accumbens, Psychopharmacology 233 (5) (2016) 831–840.
[19] B. Dubois, et al., Donepezil decreases annual rate of hippocampal atrophy in suspected prodromal Alzheimer's disease, Alzheimers Dement. 11 (9) (2015) 1041–1049.
[20] K. Rockwood, et al., Clinical meaningfulness of Alzheimer's Disease Assessment Scale-Cognitive subscale change in relation to goal attainment in patients on cholinesterase inhibitors, Alzheimers Dement. 13 (10) (2017) 1098–1106.
[21] G.R. Barker, E.C. Warburton, When is the hippocampus involved in recognition memory? J. Neurosci. 31 (29) (2011) 10721–10731.
[22] T. Ali, et al., Melatonin attenuates D-galactose-induced memory impairment, neuroinflammation and neurodegeneration via RAGE/NF-KB/JNK signaling pathway in aging mouse model, J. Pineal Res. 58 (2015) 71–85.
[23] S. Lithfous, A. Dufour, O. Despres, Spatial navigation in normal aging and the prodromal stage of Alzheimer's disease: insights from imaging and behavioral studies, Ageing Res. Rev. 12 (1) (2013) 201–213.
[24] Toru Nishinaka, C. Yabe-Nishimura, EGF receptor-ERK pathway is the major signaling pathway that mediates upregulation of aldose reductase expression under oxidative stress, Free Radic. Biol. Med. 31 (2) (2001) 205–216.
[25] B.S. Suresha, K. Srinivasan, Antioxidant potential of fungal metabolite nigerloxin during eye lens abnormalities in galactose-fed rats, Curr. Eye Res. 38 (10) (2013) 1064–1071.
[26] S.J. Tsai, M.C. Yin, Anti-oxidative, anti-glycative and anti-apoptotic effects of oleanolic acid in brain of mice treated by D-galactose, Eur. J. Pharmacol. 689 (1–3) (2012) 81–88.
[27] M. Zhang, et al., Emerging roles of Nrf2 and phase II antioxidant enzymes in neuroprotection, Prog. Neurobiol. 100 (2013) 30–47.
[28] A.D. Kraft, D.A. Johnson, J.A. Johnson, Nuclear factor E2-related factor 2-dependent antioxidant response element activation by tert-butylhydroquinone and sulforaphane occurring preferentially in astrocytes conditions neurons against oxidative insult, J. Neurosci. 24 (5) (2004) 1101–1112.
[29] D. Banji, et al., Curcumin and piperine abrogate lipid and protein oxidation induced by D-galactose in rat brain, Brain Res. 1515 (2013) 1–11.
[30] Y.F. Xian, et al., Uncaria rhynchophylla ameliorates cognitive deficits induced by D-galactose in mice, Planta Med. 77 (18) (2011) 1977–1983.
[31] J. Lu, et al., Ursolic acid attenuates D-galactose-induced inflammatory response in mouse prefrontal cortex through inhibiting AGEs/RAGE/NF-kappaB pathway activation, Cereb. Cortex 20 (11) (2010) 2540–2548.
[32] M. Kitazawa, et al., Blocking IL-1 signaling rescues cognition, attenuates tau pathology, and restores neuronal beta-catenin pathway function in an Alzheimer's disease model, J. Immunol. 187 (12) (2011) 6539–6549.
[33] T.D. Kanneganti, Central roles of NLRs and inflammasomes in viral infection, Nat. Rev. Immunol. 10 (10) (2010) 688–698.
[34] M.T. Heneka, Inflammasome activation and innate immunity in Alzheimer's disease, Brain Pathol. 27 (2) (2017) 220–222.
[35] D. Wang, et al., The role of NLRP3-CASP1 in inflammasome-mediated neuroinflammation and autophagy dysfunction in manganese-induced, hippocampal-dependent impairment of learning and memory ability, Autophagy 13 (5) (2017) 914–927.
[36] C. Juliana, et al., Non-transcriptional priming and deubiquitination regulate NLRP3 inflammasome activation, J. Biol. Chem. 287 (43) (2012) 36617–36622.
[37] Y. Song, et al., Advanced glycation end products regulate anabolic and catabolic activities via NLRP3-inflammasome activation in human nucleus pulposus cells, J. Cell. Mol. Med. 21 (7) (2017) 1373–1387.
[38] A.M. Bosch, Classical galactosaemia revisited, J. Inherit. Metab. Dis. 29 (4) (2006) 516–525.
[39] Y.N. Li, et al., Saponins from Aralia taibaiensis attenuate D-galactose-induced aging in rats by activating FOXO3a and Nrf2 pathways, Oxidative Med. Cell. Longev. 2014 (2014) 320513.
[40] Giacco, et al., Oxidative stress and diabetic complications, Circ. Res. 107 (9) (2010) 1058–1070.
[41] A.I. Rojo, et al., Deficiency in the transcription factor NRF2 worsens inflammatory parameters in a mouse model with combined tauopathy and amyloidopathy, Redox Biol. 18 (2018) 173–180.
[42] E.H. Kobayashi, et al., Nrf2 suppresses macrophage inflammatory response by blocking proinflammatory cytokine transcription, Nat. Commun. 7 (2016) 11624.
[43] E.L. Mills, et al., Itaconate is an anti-inflammatory metabolite that activates Nrf2 via alkylation of KEAP1, Nature 556 (7699) (2018) 113–117.
[44] M. Mcmahon, D.J. Lamont, K.A. Beattie, et al., Keap1 perceives stress via three sensors for the endogenous signaling molecules nitric oxide, zinc, and alkenals [J], Proc. Natl. Acad. Sci. 107 (44) (2010) 18838–18843.